Through-Ring Bonding in Edge Sharing Dimers of Octahedral Complexes

Ana A. Palacios, Gabriel Aullón, Pere Alemany, and Santiago Alvarez*

Departament de Química Inorgànica, Departament de Química Física and Centre de Recerca en Química Teòrica (CeRQT), Universitat de Barcelona, Diagonal 647, 08028 Barcelona, Spain

Received January 5, 2000

A study of the preferred structures for the M_2X_2 rings in the binuclear complexes of types $[M_2(\mu\text{-}XR_2)_2L_8]$ and $[M_2(\mu\text{-}XR_3)_2L_8]$ is presented, based on qualitative orbital arguments supported by extended Hückel calculations on Cr compounds. The main conclusions are confirmed by DFT calculations on key compounds of Cr and Mn and agree well with the results of a structural database analysis. With the simplified electron counting scheme deduced, complexes with six or four electrons available for bonding of the M_2X_2 framework are predicted to have two possible minimum energy structures, with either a short M−M or X−X distance, whereas compounds with eight framework electrons are expected to present no short through-ring distance. Such a behavior is consistent with the framework electron rules reported earlier for compounds with different coordination spheres and provides a general description of the structure and bonding in a variety of compounds with M_2X_2 diamonds. Metal−metal bonding across the ring can be equally predicted taking into account only the bonding characteristics of the t_{2g}-like orbitals for the XR_2- but not for the XR_3-bridged complexes. In addition, the framework electron counting scheme has the advantage of being independent of the formal oxidation state assigned to the metal atom.

The edge sharing bis-octahedral structure of general formula $[M_2(\mu\text{-}XR_n)_2L_8]$ is a very common pattern in the chemistry of coordination and organometallic compounds. In such a structure, two ML_4 fragments are joined by two bridging ligands that complete an octahedral coordination sphere around each metal atom (**1**).

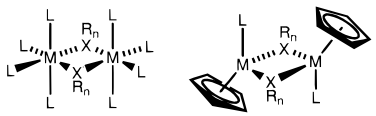

1

We include in this family those complexes with metal fragments of the type MCpL, since the η^5-cyclopentadienide ligand can be considered as electronically tridentate.[1] Not only can one find an assortment of bridging ligands of general type XR_n but also a variety of metal atoms with different oxidation states, providing different electron counts which may or may not give rise to metal−metal bonding across the ring, resulting in three possible alternative structures of the M_2X_2 framework (**2a**−**c**).

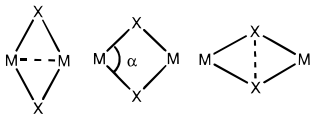

2a **2b** **2c**

In many complexes with XR_2 bridges having a d^n electron configuration of the metal atom (where $n \leq 5$), the partially occupied t_{2g} orbitals of each metal atom can account for the presence of a short through-ring metal−metal distance. The structures of complexes with XR_3 or isolobal bridging ligands (e.g., hydride) are not so easy to explain, since these bridging ligands cannot be considered as two-electron donors toward each metal atom. For analogous edge-sharing binuclear compounds of transition metal d^{10} ions with tetrahedral, or d^8 ions with square planar coordination spheres, we have shown[2,3] that a delocalized MO description results in simple electron counting rules for the M_2X_2 framework.[4] In brief, if the number of electrons available for the σ bonding of that framework is eight (framework electron count, FEC = 8), one should expect a *regular* ring, with no short distance across the ring, whereas for smaller FECs (6 or 4), a metal−metal (or a ligand−ligand) bond across the ring should be expected. Since such short through-ring distances in those cases cannot be directly associated with metal−metal bonds involving the metal d orbitals, we wish to explore the orbital analogies and differences between the bis-octahedral complexes and the previously studied binuclear structures. Our final goal is to establish simple rules to describe the bonding and structure in a wide variety of compounds with M_2X_2 cores.

A detailed study of the molecular orbital diagrams for edge-sharing bis-octahedral complexes with X or XR_2 bridges was reported early by Hoffmann and co-workers,[5] but the case of XR_3 bridges, the possibility of an alternative structure with a short X−X distance, and the changes in orbital localization that accompany the distortion of the M_2X_2 ring were not analyzed.

(1) Hoffmann, R. *Angew. Chem., Int. Ed. Engl.* **1982**, *21*, 711.
(2) Alemany, P.; Alvarez, S. *Inorg. Chem.* **1992**, *31*, 4266.
(3) Aullón, G.; Alemany, P.; Alvarez, S. *J. Organomet. Chem.* **1994**, *478*, 75.
(4) Alvarez, S.; Palacios, A. A.; Aullón, G. *Coord. Chem. Rev.* **1999**, *185*−*186*, 431.
(5) Shaik, S.; Hoffmann, R.; Fiesel, C. R.; Summerville, R. H. *J. Am. Chem. Soc.* **1980**, *102*, 4555.
(6) Mealli, C.; Orlandini, A. *Metal Clusters in Chemistry* In Braunstein, P., Oro, L. A., Raithby, P. R., Ed.; Wiley-VCH: New York, 1999; Vol. 1, p 143
(7) Rohmer, M.-M.; Bénard, M. *Organometallics* **1991**, *10*, 157.
(8) DeKock, R. L.; Peterson, M. A.; Reynolds, L. E. L.; Chen, L.-H.; Baerends, E. J.; Vernooijs, P. *Organometallics* **1993**, *12*, 2794.
(9) Janiak, C.; Silvestre, J.; Theopold, K. H. *Chem. Ber.* **1993**, *126*, 631.
(10) Cotton, F. A. *Polyhedron* **1987**, *6*, 667.

10.1021/ic000017i CCC: $19.00
Published on Web 06/28/2000

Mealli and Orlandini have also discussed in a recent paper[6] the possibility of chalcogenide coupling in electron rich M_2X_2 frameworks. Other related theoretical studies focused on specific members of these families, such as $[Zr_2(\mu\text{-}I)_2Cl_4(PH_3)_4]$[7,8] or $[Cr_2(\mu\text{-}Cl)_2Me_2Cp_2]$ and $[Cr_2(\mu\text{-}CH_3)_2Me_2Cp_2]$.[9]

Here we present a qualitative theoretical study of the bonding in the M_2X_2 rings that appear in compounds of the type $[L_4M(\mu\text{-}XR_n)_2ML_4]$, where X can be any element of the groups 14−16, M a transition element and L any ligand. We restrict our study to di- or trisubstituted bridges ($n = 2$ or 3) because in those cases it is easier to find the electron deficiency that may give rise to interesting bonding situations that cannot be explained by the formal electron configurations. A survey of edge-sharing bis-octahedral structures with X or XR bridges can be found in the literature.[10] In particular, we wish to (i) present a general MO diagram, (ii) search for possible trends in the bonding associated with the electron count, (iii) address the possible structural isomerism that may arise from the formation of X−X or M−M bonds across the ring, and (iv) provide a general description of the bonding that applies also to those complexes that cannot be accounted for by simple Lewis structures.

Our previous experience has shown us that the metal d electrons can become involved in framework bonding or remain localized at the metal atoms depending on the molecular composition and geometry.[4] Hence, for our study of the bonding within the M_2X_2 rings we find it useful to consider the total number of ring electrons provided by the bridging ligands and the metal d electrons (abbreviated NRE). We therefore assume the eight terminal ligands in the compounds studied here to be two-electron donors and exclude such electrons in the number of ring electrons. This way of counting electrons makes no a priori supposition on the bonding or electron distribution within the M_2X_2 framework, and is also independent of whether one chooses to count the bridging ligands as neutral or anionic (e.g., four electron donor R_2P^-, or three electron donor R_2P). It does not therefore depend on the formal oxidation state of the metal atom. Consider for example the compound $[Cr_2(\mu\text{-}PMe_2)_2(CO)_8]$, if we count the bridging ligands as phosphido anions, the oxidation state of the metal atoms is Cr(I), and their electron configuration d^5. If we add the 10 d electrons and the two lone pairs from each phosphido bridge, we end up with a NRE of 18. Counting the bridging ligands as neutral (thus three electrons available for bonding from each PMe group), and the chromium atoms as zerovalent (d^6), the same value of the NRE results.

We will present first the qualitative description of the electronic structure, supported by extended Hückel calculations on simple model compounds $[Cr_2(\mu\text{-}PH_2)_2L_8]$, where $L = H^-$ or CO, with different electron counts. The conclusions of our qualitative theoretical study will be used to analyze the structural data for a wide variety of compounds with general formulas $[M_2(\mu\text{-}XR_2)_2L_8]$ or $[M_2(\mu\text{-}XR_2)_2Cp_2L_2]$. In a second section we will analyze the differences introduced in the framework bonding when the bridging ligand provides only one orbital to the M_2X_2 framework, as happens with XR_3 bridges and isolobal analogues such as H^- and Ph^-. Our theoretical conclusions will be compared with the available structural data. Finally, some semiquantitative aspects of our conclusions will be confirmed by the use of the more accurate density functional calculations.

Molecular Orbitals of $[M_2(\mu\text{-}XR_2)_2L_8]$

Before analyzing the relative stability of the different structures **2a**−**c** and the differences among their electronic structures, we set up a molecular orbital diagram for the regular ring (with no short distance across the ring, **2b**), based on calculations for model chromium compounds. We expect, however, that the resulting qualitative picture should apply to other transition metals as well. The delocalized molecular orbital description of the bonding within the M_2X_2 ring can be built stepwise from the orbitals of two separate fragments M_2L_8 and X_2R_4, each having a set of antipodal atoms. These fragment orbitals can in turn be obtained as in-phase and out-of-phase combinations of the orbitals of two ML_4 (or two XR_2) groups with the appropriate symmetry. Let us start by the description of the relevant orbitals of the ML_4 fragments (**3**):

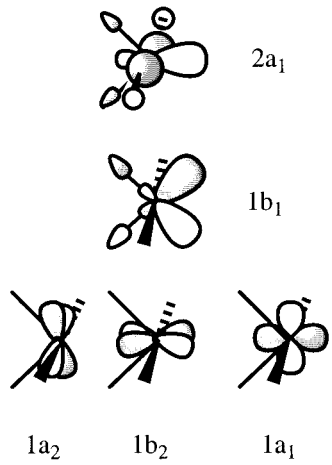

3

three of them ($1a_1$, $1a_2$, and $1b_2$, according to their symmetry in the C_{2v} point group) correspond to the t_{2g} set in the parent octahedral ML_6 complex. The other two ($2a_1$ and $1b_1$ in **3**) can be traced back to the e_g set of the parent compound, hybridized toward the missing vertices of the octahedron through mixing with the s and p orbitals of the same symmetry.[11] On the other hand, each XR_2 group has two orbitals (**4**)

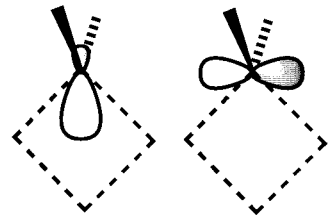

4

that can be combined to form the a_g, b_{1u}, b_{2g}, and b_{3u} orbitals of the X_2R_4 fragment that are represented in the MO diagram (Figure 1, right).

If we consider first the interaction of the e_g-type orbitals of the ML_4 fragments with the XR_2 bridges, four M−X bonding and four M−X antibonding combinations result (Figure 1). We use the greek letter φ to denote a framework bonding molecular orbital, e.g., $1b_{1u}(\varphi)$ in Figure 1. Similarly, the framework antibonding orbitals are labeled φ^* following the symmetry label of each MO. The energy ordering and bonding characteristics of the φ and φ^* orbitals are similar to those found for other complexes in which the occupied d orbitals of the transition metal do not participate in the framework bonding, such as the dimers of tetrahedral d^{10} ions.[2] The only difference is that for

(11) Albright, T. A.; Burdett, J. K.; Whangbo, W.-H. *Orbital Interactions in Chemistry*; J. Wiley: New York, 1985; p 298.

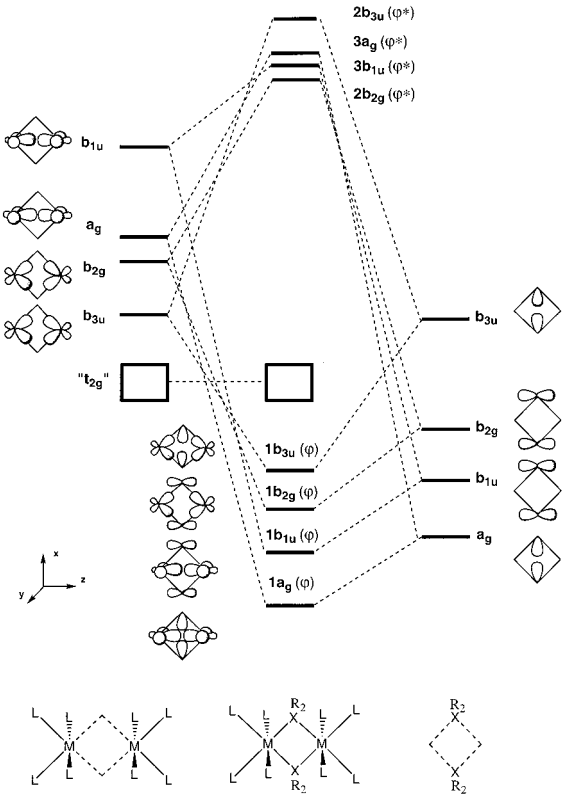

Figure 1. Qualitative MO diagram for a binuclear complex $[M_2(\mu\text{-}XR_2)_2L_8]$, represented as resulting from the interaction between M_2L_8 and $(XR_2)_2$ fragments at $\alpha \approx 90°$ (**2b**), using the symmetry labels of the D_{2h} point group. The t_{2g}-block orbitals are depicted in **5**.

tetrahedral ions the φ orbitals are built up of metal s and p orbitals of the appropriate symmetry instead of d orbitals.

Next, we need to analyze how the t_{2g}-block orbitals change from the ML_4 fragments to the binuclear molecule. In the regular ring the metal−metal distance is too large for direct overlap between the d orbitals, and only the interactions with the bridge orbitals are relevant, but in a distorted ring with short metal−metal distance the direct overlap becomes important. The symmetry-adapted combinations of the t_{2g}-block orbitals are shown in **5**,

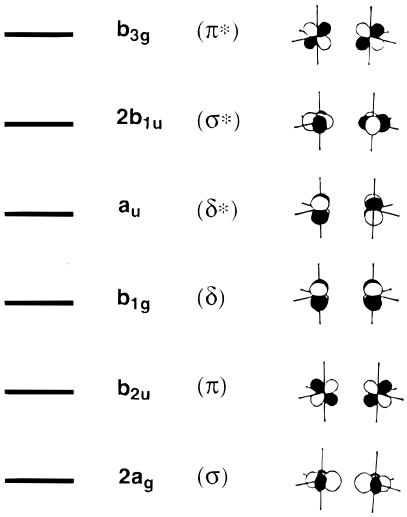

5

together with their symmetry label and their metal−metal bonding characteristics. Of these orbitals, only $2a_g$ and $2b_{1u}$ are allowed by symmetry to interact with the bridges. But mixing of $2a_g$ with the bridges is small and it is only slightly destabilized, preserving its t_{2g} character. Therefore, we label this MO as $2a_g(t_{2g})$. In the case of the $2b_{1u}$ orbital in **5**, through interaction with the bridge orbitals of the same symmetry (Figure 2), all the M−X bonding character is concentrated in $1b_{1u}(\varphi)$ and the M−X antibonding character in $3b_{1u}(\varphi^*)$, whereas the t_{2g}-like orbital is only slightly destabilized and remains as formally M−X nonbonding, hence we label this orbital as $2b_{1u}(t_{2g})$. The most relevant result is that the low-lying orbital, $1b_{1u}(\varphi)$, has its contribution at the metal atom hybridized away from the ring, thus losing the σ^*(M−M) character expected when mixing between t_{2g} and φ orbitals is not considered (Figure 1). Conversely, $2b_{1u}(t_{2g})$ is hybridized inward and has a marked σ^*(M−M) character. Hence, it is slightly above the rest of the t_{2g}-block, and its energy is expected to be highly sensitive to the M−M distance. In summary, $1b_{1u}(\varphi)$ retains its framework bonding nature, but loses its σ^*(M−M) character, whereas $2b_{1u}(t_{2g})$ concentrates most of the σ^*(M−M) characteristics, and $3b_{1u}(\varphi^*)$ retains its framework antibonding nature. Although we have labeled the b_{1u} orbitals according to their φ, t_{2g} or φ^* characteristics, we show below that the composition of these MOs is modified when the ring is distorted from the regular geometry.

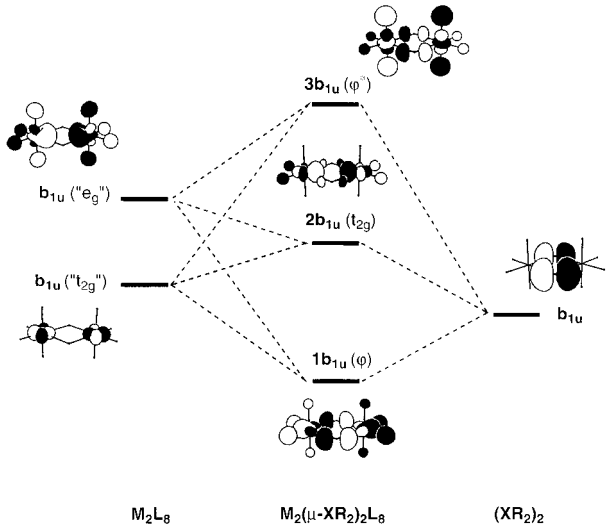

Figure 2. Rehybridization of the b_{1u} orbitals of the t_{2g}-block after mixing with orbitals of the same symmetry from the bridging ligands.

For the subsequent discussion it is important to analyze how the $2b_{1u}$ orbital evolves upon ring squeezing in either direction ($\alpha > 90°$ or $\alpha < 90°$, see **2**). At sufficiently long M−M distances (**2b** or **2c**), this orbital has mostly t_{2g} character as discussed above, but as α increases it becomes more delocalized and strongly M−X bonding (i.e., φ-like in **2a**). Conversely, $1b_{1u}$ is strongly M−X bonding (φ-like) at small α but more localized at the metal atom (t_{2g}-like) at large α. Taking into account the variable nature of the b_{1u} orbitals, we will omit their identification as φ, t_{2g} or φ^* from here on, and label them simply as $1b_{1u}$, $2b_{1u}$ and $3b_{1u}$. The exchange of the φ and σ^*(M−M) character of two of these orbitals upon ring deformation is illustrated in Figure 3 and has important consequences for the bonding and stability in the three different forms of these compounds (**2**), as discussed below.

Now we can build an idealized Walsh diagram for the ring distortion (Figure 4), taking into account the discussion above, and also considering the strong σ^*(X−X) antibonding character of $1b_{3u}(\varphi)$ at small angles. With such a diagram we can try to predict the most stable structures for different electron counts.

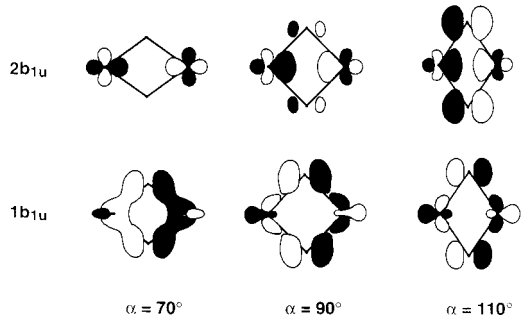

Figure 3. Rehybridization of the $1b_{1u}$ and $2b_{1u}$ orbitals resulting from distortion of the M_2X_2 ring in $[M_2(\mu\text{-}XR_2)_2L_8]$. The values of α given correspond approximately to structures **2c** (α = 70°), **2b** (α = 90°), and **2a** (α = 110°).

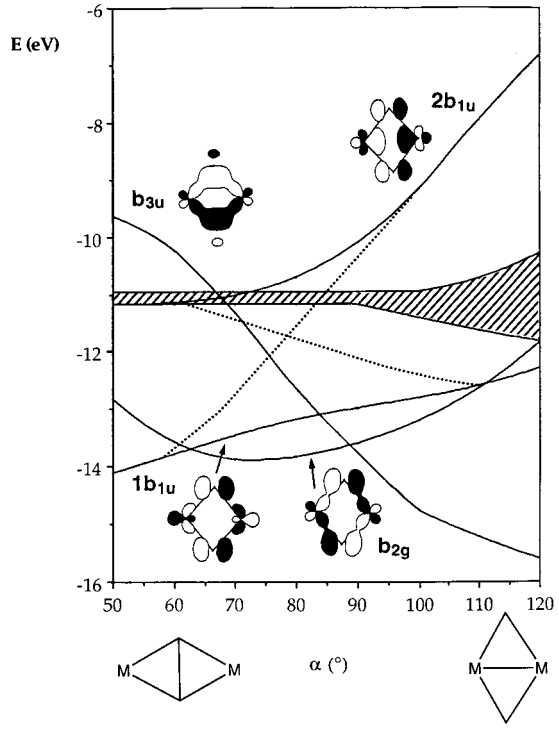

Figure 4. Walsh diagram for the framework bonding orbitals and t_{2g}-block orbitals in a binuclear complex $[M_2(\mu\text{-}XR_2)_2L_8]$ as a function of the ring distortion measured by α (see **2**). The lowest orbital, $1a_g(\varphi)$, is omitted for simplicity.

Although we cannot expect EH calculations to provide accurate estimates of bond distances, we have optimized the Cr−Cr bond distance of our model complex for different electron configurations while keeping all the metal−ligand distances frozen (Table 1). We expect these results to give us a qualitative idea of the way in which these may be affected by the occupation of the valence orbitals. Since we wish to rationalize the structures of compounds with different metal and bridging atoms, we will consider from here on the difference between the through-ring M···M distance and the sum of the atomic radii: $\Delta_{MM} = d(M-M) - 2r_M$. Such a bonding parameter is more comparable for different metals than the M−M distances, although the actual values depend on the choice of a set of atomic radii. The most salient feature of our results is the persistence of short Cr−Cr distances (Table 1), which correspond to $\Delta_{CrCr} \leq 0.23$ Å (r_{Cr} = 1.42 Å), i.e., a structure of type **2a**, for any electron count that leaves the $2b_{1u}$ orbital empty (NRE ≤ 18 with low spin configuration). When that orbital is occupied (NRE = 20), no Cr−Cr bond is expected due to its σ^*(M−M) nature, and a long distance is predicted ($\Delta_{CrCr} \geq 0.31$ Å, structure **2b**).

Table 1. Through-Ring Distances (angstroms) in the Calculated (EH) Minima of the $[Cr_2(\mu\text{-}XH_2)_2L_8]$ Complexes with Different Number of Ring Electrons (NRE) for Their Singlet State

	M−M in **2a**			X−X in **2c**		
NRE	X = P, L = H	X = P, L = CO	X = N, L = CO	X = P, L = H	X = P, L = CO	X = N, L = CO
6	2.944	2.756	2.889	2.175	2.115	1.561
8	3.076	3.108	2.916	2.175	2.122	1.560
10	2.970	3.010	2.705	2.168	2.115	1.550
12	2.811	3.029	2.751	2.163	2.113	1.545
14	2.768	3.012	2.620	2.170	2.148	1.561
16	2.808	2.941	2.603	2.178	2.108	1.555
18	2.964	3.072	2.838	2.201	2.112	1.556

M−M in **2b**[a]

NRE	X = P, L = H	X = P, L = CO	X = N, L = CO
20	3.402	3.515	3.150

[a] No minima of structures **2a** or **2c** were found for NRE = 20.

The previous qualitative discussion was substantiated by EH calculations on simple model compounds $[Cr_2(\mu\text{-}PH_2)_2H_8]^{y-}$. Similar results have been obtained with the more realistic terminal ligands and different bridging ligands in $[Cr_2(\mu\text{-}XH_2)_2(CO)_8]^{y-}$, where X = N or P. The substitution of the PH_2 bridges by NH_2 groups results in shorter Cr−Cr distances, a result that can be traced back to the shorter Cr-X bond distance that produces a stronger destabilization of those orbitals with σ^* or π^* character upon increasing α (see Table 1). If the terminal ligands are substituted by chloride ions, a similar Walsh diagram is obtained, but the calculated Cr−Cr distances at the minimum when NRE ≤ 18 are significantly longer (e.g., 3.402 Å for NRE = 14, compared to 3.012 Å with L = CO). Such a longer distance is due to chloride···chloride repulsions, as revealed by a population analysis, and agrees with previous findings for related molecules with unsubstituted bridges.[5,12]

Given the small energy separation between the t_{2g}-block orbitals (with the exception of $2b_{1u}$), one should expect high spin configurations to be more stable than the low spin one. In the case of bis{(μ-diethylamido)-bis(*N*,*N*-diethylcarbamato)-chromium(III)},[13] for instance, the magnetic moment at room temperature is 2.28 μ_B, indicating that the structural data correspond to thermally populated low spin and intermediate spin states (i.e., weakly antiferromagnetically coupled metal ions).

As found previously for analogous systems with other ML_n fragments,[2,3] a second energy minimum is also found at short X−X distance (**2c**) for all electron counts between 6 and 18, but not for NRE = 20. The number of ring electrons affects only the occupation of the t_{2g}-type orbitals, which have little bearing on X−X bonding. Hence, the calculated X−X distance in structure **2c** is practically independent of the electron count (Table 1), in contrast with the dependence predicted for the M−M distance in structure **2a**. It must be noted, however, that structure **2a** is predicted to be in all cases more stable than **2c**, with a rather small barrier for the conversion of **2c** into **2a**. A more accurate evaluation of the relative stabilities for systems with NRE = 18 or 20, carried out with the help of density functional calculations, will be presented below.

No short X−X distances can be found among the structural data for edge-sharing octahedra with XR_2 bridges (Table S1,

(12) Poli, R.; Torralba, R. C. *Inorg. Chim. Acta* **1993**, *212*, 123.
(13) Chisholm, M. H.; Cotton, F. A.; Extine, M. W.; Rideout, D. C. *Inorg. Chem.* **1978**, *17*, 3536.

Supporting Information), in agreement with the lower stability predicted for this form. To see if there is a way to stabilize the structure **2c** relative to **2a**, we can make use of the Walsh diagram (Figure 4). Since **2c** is destabilized by the b_{3u} orbital and stabilized by $1b_{1u}$, the appropriate electron configuration is one with the former orbital empty and the latter occupied. This can in principle be achieved for NRE $\leq$ 6, corresponding formally to d^0 metal ions with bridges providing up to three electrons each. Calculations on our simple chromium model compound indicate that structure **2c** is more stable than **2a** by 2 kcal/mol in that case. Actually, one can find such structures ($\Delta_{XX} \approx 0$) for compounds with NRE = 6 and CH_2 bridges, but only with ML_5, ML_6 or ML_7 fragments so far.[15−19] This is no surprise, since such low electron counts can only be achieved with d^0 or d^1 electron configurations for the metal ions, which would be highly coordinatively unsaturated with only four terminal ligands. Also related Zr(II) compounds with N_2 bridges have been reported by Fryzuk and co-workers.[20,21] Interestingly, if one considers each bridging N atom to have two electron pairs directed away from the Zr_2N_2 ring in sp^3 hybrids, one is left with a total of six ring electrons for the framework and t_{2g} orbitals and, according to the above discussion, a short N−N distance should be expected, as experimentally found (1.53−1.55 Å, compared to 1.098 Å in free N_2 or to 1.45 Å for a single N−N bond). In contrast, a related calixarene Nb(III) complex with nitrido bridges has NRE = 12, and a short Nb−Nb distance has been reported (2.800 Å, Δ_{MM} = 0.06 Å).[22] Finally, a related chromium compound with a bridging disulfide[23] must be noted.

Complexes Bridged by XR_3 or Isolobal Groups

Since it was previously found[2] that bridging groups with only one orbital available for framework bonding, such as Me, hydride, pyridine, or Ph, behave differently than those fragments with two or more lobes, we need to separately discuss the bonding and electronic structure in this case, using qualitative arguments supported by EH calculations on $[Cr_2(\mu\text{-}CH_3)_2H_8]^{y-}$. Similar results were obtained with NH_3 or CO as terminal ligands. However, if Cl^- was used as terminal ligand, the Cr−Cr distances appeared to be significantly longer due to enhanced steric repulsions when the two metal atoms approach. Steric repulsions can be identified via a population analysis between the axial ligands of the two metal atoms (as seen above for compounds with XR_2 bridges), and between equatorial terminal and bridging ligands.

The main difference between the resulting interaction diagram for a regular rhombus with XR_3 bridges (Figure 5) and that previously discussed for XR_2 bridges (Figure 1) stems from the fact that the bridging ligands contribute only one orbital each to the framework bonding. Hence, the b_{2g} and b_{1u} orbitals of the metal fragments remain now M−X non bonding. One is left then with only two framework bonding orbitals, $1a_g(\varphi)$ and $1b_{3u}(\varphi)$, and their antibonding counterparts, $3a_g(\varphi^*)$ and $2b_{3u}(\varphi^*)$. The b_{2g} and $2b_{1u}$ orbitals are now purely metal−metal π- and σ-antibonding, respectively, and the t_{2g} block remains nonbonding, with only the combination that has σ^*_{MM} character, $1b_{1u}(t_{2g})$, slightly destabilized due to mixing with the bridging ligands. With such an orbital scheme, it is clear that the M_2X_2 framework for these systems must be electron deficient, since the maximum possible bond order is two for four M−X linkages.

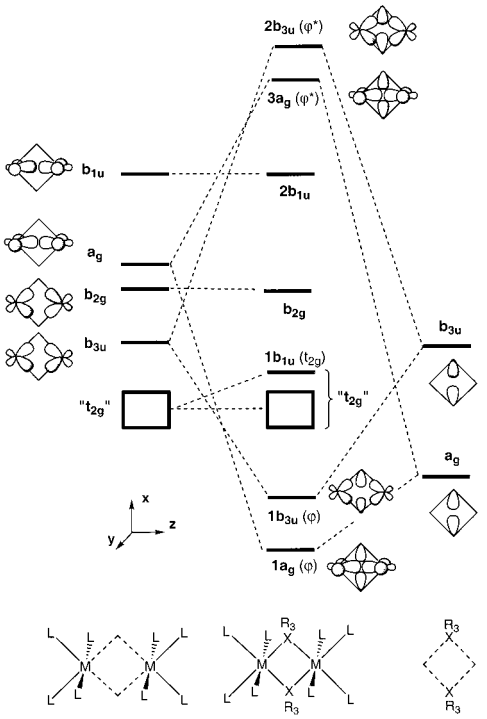

Figure 5. Qualitative MO diagram for a binuclear complex $[M_2(\mu\text{-}XR_3)_2L_8]$, represented as resulting from the interaction between M_2L_8 and $(XR_3)_2$ fragments at $\alpha \approx 90°$ (**2b**). The t_{2g} block orbitals are schematically depicted in **5**.

With such an MO diagram at hand one sees that the two framework bonding orbitals, $1a_g(\varphi)$ and $1b_{3u}(\varphi)$ have M−M bonding character. These orbitals are occupied for any number of ring electrons (NRE) from four up. Since the M−M antibonding counterparts, $1b_{2g}$ and $2b_{1u}$ are empty for electron counts up to NRE = 16, one should expect a net bonding M−M interaction through the ring for all values of NRE between 4 and 16. The two lowest occupied orbitals have framework bonding character, and the M_2X_2 framework may still be stable. However, comparison with the case discussed above, in which there are four M−X bonding orbitals, suggests that the M−X bonds should be weaker in the present case. Unfortunately, there are no structurally characterized compounds with the same metal and bridging atoms having different number of substituents to verify such a prediction, but we will come back to this issue in the next section.

A look at the calculated Cr−Cr distances for the model compounds (Table 2) confirms the qualitative prediction, since all such distances are in this case shorter than 3.2 Å, in contrast with the longer distances calculated for analogous complexes with XR_2 bridges and NRE = 20 (Table 1). Of course, for NRE = 16, the occupation of $1b_{1u}(t_{2g})$ with M−M antibonding

(14) Rohmer, M.-M.; Bénard, M.; Cadot, E.; Secheresse, F. In *Polyoxometalates: From Topology to Industrial Applications*; Müller, A., Pope, J. T., Eds.; Kluwer: Dordrecht. In press.
(15) Cotton, F. A.; Kibala, P. A. *Inorg. Chem.* **1990**, *29*, 3192.
(16) Horng, K. M.; Wang, S. L.; Liu, C. S. *Organometallics* **1991**, *10*, 631.
(17) Fernández, F. J.; Gómez-Sal, P.; Manzanero, A.; Royo, P.; Jacobsen, H.; Berke, H. *Organometallics* **1997**, *16*, 1553.
(18) Burns, C. J.; Andersen, R. A. *J. Am. Chem. Soc.* **1987**, *109*, 915.
(19) Dubé, T.; Gambarotta, S.; Yap, G. P. A. *Angew. Chem., Int. Ed. Engl.* **1999**, *38*, 1432.
(20) Fryzuk, M. D.; Haddad, T. S.; Rettig, S. J. *J. Am. Chem. Soc.* **1990**, *112*, 8185.
(21) Cohen, J. D.; Fryzuk, M. D.; Loehr, T. M.; Mylvaganam, M.; Rettig, S. J. *Inorg. Chem.* **1998**, *37*, 112.
(22) Zanotti-Gerosa, A.; Solari, E.; Giannini, L.; Floriani, C.; Chiesi-Villa, A.; Rizzoli, C. *J. Am. Chem. Soc.* **1998**, *120*, 437.
(23) Herrmann, W. A.; Rohrmann, J.; Noth, H.; Narula, C. K.; Bernal, I.; Draux, M. *J. Organomet. Chem.* **1985**, *284*, 189.

Table 2. Calculated (EH) Cr−Cr Distances (angstroms) for CH_3-Bridged Chromium Compounds with Different Numbers of Ring Electrons (NRE) and Spin States, and Experimental Data for the Related Cr Compound

NRE	compound	*S*	calcd M−M	exptl M−M
4	$[Cr_2(\mu\text{-}CH_3)_2(CO)_8]^{10+}$	0	3.053	
10	$[Cr_2(\mu\text{-}CH_3)_2(CO)_8]^{4+}$	0	2.741	
		2	2.871	
		3	3.131	
10	$[Cr_2(\mu\text{-}CH_3)_2(CH_3)_2Cp_2]$	0	2.834	
		2	2.954	
		3	3.137	
	$[Cr_2(\mu\text{-}CH_3)_2(CH_3)_2Cp^*_2]$[24]	*a*		2.606
16	$[Cr_2(\mu\text{-}CH_3)_2(CO)_8]^{2-}$	0	3.199	

[a] $\mu_{ef} = 2.1\ \mu_B$.

character, results in a distance longer than for other electron counts, but still much shorter than found for structure **2b** with XR_2 bridges (larger than 3.7 Å, Table 3), suggesting that most of the metal−metal antibonding is concentrated in the $2b_{1u}$ orbital, while $1b_{1u}$ remains formally non bonding. The experimental structural data found for complexes with alkyl or hydride bridges (Table S2, Supporting Information) are in excellent agreement with our qualitative predictions: in all cases the M−M distance is close to or smaller than the atomic radii sum. An additional corollary of the molecular orbital diagram for compounds with trisubstituted bridges (Figure 5) is that the structure **2c** with short X−X distance is not a minimum in the potential energy surface, in contrast to the results for XR_2 bridges. To obtain a short X−X distance one needs to empty the $1b_{3u}$ orbital, but this would leave the ring with only one pair of bonding electrons and the M_2X_2 framework is expected to fall apart. Consistently, a minimum of type **2c** has not been found in our EH calculations, and no experimental structure of that type has been reported. However, the possibility of such a structure appearing as a transition state in ligand coupling reactions seems an interesting hypothesis and probably deserves further study.

Two features of the MO diagram (Figure 5) are worth being stressed. First, given the small separation between the t_{2g} orbitals, one should probably expect that configurations with unpaired electrons are more stable than the $S = 0$ configurations for electron counts $6 \le NRE \le 14$. Second, the separation between the highest t_{2g} MO, $1b_{1u}(t_{2g})$, with σ^* metal−metal character, and the rest of the t_{2g} block should probably result in that orbital being empty for $NRE \le 14$. As in the case of the XR_2 bridges, different occupations of the t_{2g} block orbitals should result in different metal−metal distances, but also different spin states of the same configuration may be expected to give different distances (see Table 2). The only chromium compound of this family whose structure has been reported so far fits nicely into the picture, with an antiferromagnetic behavior ($\mu_{eff} = 2.1\ \mu_B$ at room temperature) and a short Cr−Cr distance, consistent with the presence of thermally populated $S = 2$ and $S = 0$ states at room temperature. In this context, it is also interesting to recall the structure of $[Cp^*_2Cl_2Ru_2(\mu\text{-}Cl)_2]$ in which two different Ru_2Cl_2 rings coexist, with one short and one long Ru−Ru distance, consistent with low spin and high-spin configurations, respectively.[25]

Since we claim that the short metal−metal distance in the M_2X_2 diamonds is mostly due to the delocalized bonding of the framework orbitals (φ in this paper), it is interesting to analyze in the present case the importance of the t_{2g} orbitals for the metal−metal bonding. To that end we have carried out a Mulliken population analysis for the $S = 2$ state of $[Cr_2(\mu\text{-}CH_3)_2(CO)_8]^{4+}$, which has been seen to reasonably represent the electronic structure of the experimentally characterized $[Cr_2(\mu\text{-}CH_3)_2(CH_3)_2Cp^*_2]$. For such a model compound, the Cr−Cr overlap population at 2.871 Å is 0.135. The contribution of the φ orbitals to that overlap population is 0.120, whereas that of the t_{2g} block is only 0.024 and a smaller negative contribution comes from low lying molecular orbitals. These results clearly indicate that there is some contribution of the t_{2g} orbitals to Cr−Cr bonding, but most of that bonding comes from the delocalized interaction of the four atoms in the Cr_2C_2 ring. Similar results are obtained for the $S = 0$ and $S = 3$ states, and only in the former case the contribution of the t_{2g} orbitals to the Cr−Cr bonding is significant, amounting to approximately one-third of the total overlap population.

Density Functional Calculations for $[Cr_2(\mu\text{-}PH_2)_2(CO)_8]^{y-}$ ($y = 0, 2$)

In this section we present the results of density functional (DFT) calculations for compounds of formula $[Cr_2(\mu\text{-}PH_2)_2(CO)_8]^{y-}$, corresponding to NRE = 18 ($y = 0$) and NRE = 20 ($y = 2$), and $[Mn_2(\mu\text{-}SiH_2)_2(CO)_8]$ (NRE = 18). The optimized through-ring distances, together with the pertinent experimental structural data, are presented in Table 3.

Table 3. Results of Density Functional (B3LYP) Calculations for $[Cr_2(\mu\text{-}PH_2)_2(CO)_8]^{y-}$ and $[Mn_2(\mu\text{-}SiH_2)_2(CO)_8]^{y-}$ ($y = 0$ and 2, corresponding to NRE = 18 and 20, Respectively), Together with Experimental Data for Related Compounds[a] of Cr and Mn

NRE	compound		structure	M−M	X−X	M−X	R−X-R	L_{eq}−M−L_{eq}	refcode	ref.
14	$[Cr_2(\mu\text{-}NEt_2)_2(O_2CNEt)_4]$		**2a**	2.948	2.836	2.045	112.8	86.7	eacbct	13
14	$[Cr_2(\mu\text{-}NR_2)_2Cl_3]$[b]		**2a**	2.981	2.791	2.103	106.6	96.1	yeffeu	26
18	*trans*-$[Cr_2(\mu\text{-}NMe)_2Cp_2(NO)_2]$		**2a**	2.670	2.950	1.990	102.7		macpct10	27
	cis-$Cr_2(\mu\text{-}NMe)_2Cp_2(NO)_2]$		**2a**	2.719	2.970	2.014	103.0		macpcc10	27
	$[Cr_2(\mu\text{-}AsMe_2)_2(CO)_8]$		**2a**	2.995	3.807	2.422	102.3	86.0	mascrd	28
	$[Cr_2(\mu\text{-}PMe_2)_2(CO)_8]$		**2a**	2.904	3.614	2.318	102.0	91.4	mpcrco	29
	$[Cr_2(\mu\text{-}PH_2)_2(CO)_8]$ calcd.	($S = 0$)	**2a**	3.044	3.710	2.400	100.4	88.2		
		($S = 1$)	**2a**	3.510	3.741	2.565	99.2	89.0		
	$[Cr_2(\mu\text{-}PH_2)_2(CO)_8]$ calcd.	($S = 0$)	**2c**	4.742	2.270	2.629	121.8	93.9		
		($S = 1$)	**2c**	4.235	2.844	2.551	107.9	93.2		
	$[Mn_2(\mu\text{-}SiH_2)_2(CO)_8]$ calcd.	($S = 0$)	**2a**	2.956	3.828	2.418	106.4	95.8		
	$[Mn_2(\mu\text{-}CF_2)_2(CO)_8]$		**2a**	2.664	3.076	2.034	102.7	95.4	dofpet	30
	$[Mn_2(\mu\text{-}SiPh_2)_2(CO)_8]$		**2a**	2.871	3.852	2.402	-[c]	96.4	dpscmn	31
	$[Mn_2(\mu\text{-}SiH_2)_2(CO)_8]$ calcd.	($S = 0$)	**2c**	4.614	2.362	2.592	119.2	95.8		
20	$[Cr_2(\mu\text{-}SEt_2)_2(CO)_8]$		**2b**	3.788	3.020	2.422	102.0	91.0	denhej	32
	$[Cr_2(\mu\text{-}PH_2)_2(CO)_8]^{2-}$ calcd.	($S = 0$)	**2b**	4.056	3.082	2.547	95.3	94.1		
	$[Mn_2(\mu\text{-}SiH_2)_2(CO)_8]^{2-}$ calcd.	($S = 0$)	**2b**	4.034	2.987	2.510	101.9	100.5		

[a] All distances in angstroms, angles in degrees. [b] One tridentate $N\{(CH_2)_2PMe_2\}_2$ ligand and one tetradentate $Me_2P(CH_2)_2N(CH_2)_2PMeCH_2$ ligand. [c] One phenyl group is disordered.

Table 4. Relative Energies (kcal/mol) of Structures 2a and 2c of $[Cr_2(\mu\text{-}PH_2)_2(CO)_8]$ in the Singlet and Triplet States (NRE = 18), and of $[Mn_2(\mu\text{-}SiH_2)_2(CO)_8]$ in the Singlet State, as Obtained through DFT Calculations

M	state	2a	2c
Cr	$S = 0$	0.0	96.4
Cr	$S = 1$	51.9	73.2
Mn	$S = 0$	0.0	36.4

The results of the DFT calculations for the Cr compound with NRE = 18 confirm the qualitative conclusions of the discussion in the preceding section, in the sense that two minima corresponding to structures **2a** and **2c** are found both for the singlet and triplet states. The structure with a short Cr···Cr distance (**2a**) is found to be the most stable one in its singlet state (Table 4). The minimum with a short P···P distance (**2c**) is much higher in energy and appears to be more stable in its triplet state. The analysis of the Kohn−Sham orbitals for the optimized structures is fully consistent with the Walsh diagram presented above (Figure 4), the LUMO being $2b_{1u}$ and b_{3u} for structures **2a** and **2c**, respectively. Also the relative energies of the singlet and triplet states predicted for **2a** and **2c** are in agreement with the different HOMO−LUMO gaps expected from the EH calculations.

The interpretation of the differences in structural parameters calculated for $[Cr_2(\mu\text{-}PH_2)_2(CO)_8]$ (Table 3) is straightforward if one takes into account the occupation of the molecular orbitals in each case. The partially occupied orbitals in the triplet state are $1b_{2g}$ and $2b_{1u}$ for **2a**, $1b_{3u}$ and $2b_{1u}$ for **2c** (see Figures 1 and 2). A linear dependence can be found between the optimized X···X distance and the occupation of the $1b_{3u}$ orbital with σ^*-(X···X) character. A dependence of the Cr···Cr distance on the occupation of the $2b_{1u}$ orbital can also be found, even if slightly perturbed in the triplet states by the occupation of $1b_{2g}$ and $1b_{3u}$ (of Cr···Cr π^* and π character, respectively).

It is noteworthy that the C−Cr−C and H−P−H bond angles are very sensitive to the structure adopted by the Cr_2P_2 core of $[Cr_2(\mu\text{-}PH_2)_2(CO)_8]$. The two angles are larger in the isomer with a short P−P through-ring distance, and a good correlation can be found between the C−Cr−C and P−Cr−P bond angles. These results can be rationalized by considering different contributions of two resonance structures, one with octahedrally coordinated Cr atoms and tetrahedrally coordinated bridging atoms (**6a**),

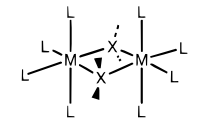

6a

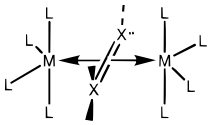

6c

and one with a double bonded $R_2P{=}PR_2$ ligand coordinated in a η^2 fashion to the two Cr atoms, which thus have a trigonal bipyramidal coordination sphere (**6c**).[3]

To check that our qualitative conclusions apply to other transition metal atoms, we carried out similar calculations on the model Mn compound with SiH_2 bridges and NRE = 18, and the results (Tables 3 and 4) are fully consistent with those discussed above for the isoelectronic Cr phosphido-bridged complex. The existence of a short Mn−Mn distance is consistent with the experimental values for the isoelectronic complexes (Table 3) and the calculated bond distances and angles are in excellent agreement with those reported for $[Mn_2(\mu\text{-}SiPh_2)_2(CO)_8]$.[31] In contrast, phosphido-bridged Mn species with NRE = 20[29,33−40] present Mn−Mn distances longer than 3.67 Å.

The conclusion of our qualitative analysis above that only one minimum with structure **2b** can be found for NRE = 20 is also supported by the DFT results on $[Cr_2(\mu\text{-}PH_2)_2(CO)_8]^{2-}$, for which the optimized structural data can be found in Table 3. In summary, the optimized structure for the model chromium and manganese complexes with NRE = 18 or 20 are in qualitative agreement with the above EH calculations and in excellent agreement with the values experimentally found. A DFT study of the analogous Fe, Ru, and Os compounds with SiR_2 bridges is under way in our group, and the results for such complexes with NRE = 18 or 20 are also consistent with the above qualitative picture and with the available experimental data.

Comparison with Experimental Structures

The experimental Δ_{MM} values (data and refcodes provided as Supporting Information) for the two families of compounds considered in this paper can be compared to the theoretical values discussed above (Figure 6). An excellent qualitative agreement is found between the results of the model calculations on chromium compounds and the experimental data for either chromium or other transition metal complexes: In general, compounds with NRE of 18 or less present metal−metal distances that exceed the atomic radii sum by at most 0.3 Å, whereas compounds with NRE of 20 have metal−metal distances in excess of 0.3 Å above the atomic radii sum. Another trend that can be observed is that the chromium compounds with amido bridges present shorter Cr−Cr distances than those with phosphido bridges (Table S1, Supporting Information), in excellent agreement with our computational results.

It is interesting to note that in three compounds two donor atoms of a porphyrin[41] or porphycenato[42] ring act as bridges between Tc or Re atoms and the other two occupy an axial position of each metal atom. The bridging N atoms contribute to the framework bonding with only their σ-type lone pairs,

(24) Noh, S.-K.; Sendlinger, S. C.; Janiak, C.; Theopold, K. H. *J. Am. Chem. Soc.* **1989**, *111*, 9127.
(25) Kölle, U.; Kossakowski, J.; Klaff, N.; Wesemann, L.; Englert, U.; Heberich, G. E. *Angew. Chem., Int. Ed. Engl.* **1991**, *30*, 690.
(26) Al-Soudani, A.-R. H.; Batsanov, A. S.; Edwards, P. G.; Howard, J. A. K. *J. Chem. Soc., Dalton Trans.* **1994**, 987.
(27) Bush, M. A.; Sim, G. A. *J. Chem. Soc. A* **1970**, 611.
(28) Vahrenkamp, H.; Keller, E. *Chem. Ber.* **1979**, *112*, 1991.
(29) Vahrenkamp, H. *Chem. Ber.* **1978**, *111*, 3472.
(30) Schulze, W.; Hartl, H.; Seppelt, K. *Angew. Chem., Int. Ed. Engl.* **1986**, *25*, 185.
(31) Simon, G. L.; Dahl, L. F. *J. Am. Chem. Soc.* **1973**, *95*, 783.
(32) Bremer, G.; Klufers, P.; Kruck, T. *Chem. Ber.* **1985**, *118*, 4224.
(33) Masuda, H.; Taga, T.; Machida, K.; Kawamura, T. *J. Organomet. Chem.* **1987**, *331*, 239.
(34) Deppisch, B.; Schafer, H.; Binder, D.; Leske, W. *Z. Anorg. Allg. Chem.* **1984**, *519*, 53.
(35) Flörke, U.; Haupt, H.-J. *Acta Crystallogr., Sect. C: Cryst. Struct. Commun.* **1993**, *49*, 374.
(36) Flörke, U.; Haupt, H.-J. *Acta Crystallogr., Sect. C: Cryst. Struct. Commun.* **1993**, *49*, 533.
(37) Brown, M. P.; Buckett, J.; Harding, M. M.; Lynden-Bell, R. M.; Mays, M. J.; Woulfe, K. W. *J. Chem. Soc., Dalton Trans.* **1991**, 3097.
(38) Flörke, U.; Haupt, H.-J. *Z. Kristallogr.* **1996**, *211*, 333.
(39) Flörke, U.; Haupt, H.-J. *Z. Kristallogr.* **1996**, *211*, 335.
(40) Manojlovic-Muir, L.; Muir, K. W.; Jennings, M. C.; Mays, M. J.; Solan, G. A.; Woulfe, K. W. *J. Organomet. Chem.* **1995**, *491*, 255.
(41) Tsutsui, M.; Hrung, C. P.; Ostfeld, D.; Srivastava, T. S.; Cullen, D. L.; Meyer, E. F., Jr. *J. Am. Chem. Soc.* **1975**, *97*, 3952.
(42) Che, C.-M.; Li, Z.-Y.; Guo, C.-X.; Wog, K.-Y.; Chern, S.-S.; Peng, S.-M. *Inorg. Chem.* **1995**, *34*, 984.

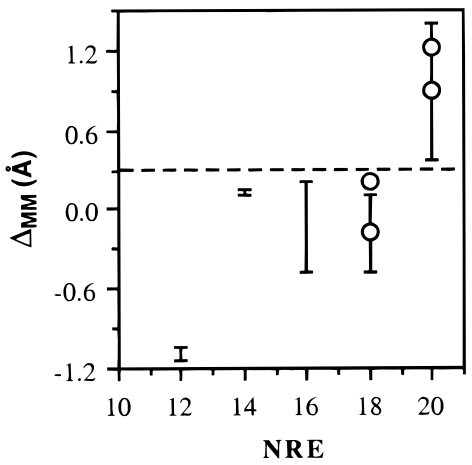

Figure 6. Experimental ranges for the difference between the M−M distance and the atomic radii sum, Δ_{MM} in transition metal complexes of the type $[M_2(\mu\text{-}XR_n)_2L_8]$ ($n = 2$, 3) as a function of the number of ring (vertical lines). Values calculated at the B3LYP level for model compounds $[M_2(\mu\text{-}XR_n)_2(CO)_8]^{y-}$ (M = Cr, X = P; M = Mn, X = Si; $y = 0$, 2) in their most stable geometry with the low spin state (Tables 3 and 4) are also shown (circles).

given its sp^2 hybridization and the involvement of p_π lone pair in the π system of the aromatic ring. These bridging ligands are thus isolobal with an XR_3 bridge and the resulting number of ring electrons is 16, for which short metal−metal distances are expected, as experimentally found (Δ_{MM} values of at most 0.21 Å).

Conclusions and Outlook

The framework molecular orbitals (φ) of the edge-sharing $[M_2(\mu\text{-}XR_2)_2L_8]$ complexes with a regular M_2X_2 ring are essentially formed by the combination of e_g-like d orbitals of the ML_4 fragments and the symmetry-adapted combinations of the bridging ligand lone pair orbitals. Upon ring distortion, the b_{1u} orbitals change their characteristics: $2b_{1u}$ (with metal−metal σ^* character) is metal-centered (t_{2g}-like) at long M···M distances, but is increasingly delocalized at short M···M distances, incorporating M−X bonding character.

A qualitative orbital analysis indicates that, for all electron configurations having the lowest three φ orbitals occupied and $2b_{1u}$ empty, a short metal−metal distance should be expected across the ring. These qualitative predictions are confirmed by DFT calculations for model complexes with a number of ring electrons (NRE) of 18 and 20. Adopting a simplified model in which the MOs are described by their approximate composition in the ring with long M···M distance, the first six ring electrons occupy framework bonding orbitals, then the six t_{2g}-block orbitals are occupied, and finally the fourth φ orbital is filled. Therefore, one could formally assign a framework electron count (FEC) of six for all electron counts $6 \le NRE \le 18$, and a FEC of eight for NRE = 20. Within such a counting scheme, the rules for predicting the geometry of the M_2X_2 framework are the same previously described for M_2X_2 frameworks with different coordination environments around the metal atoms: short metal−metal distances are predicted for FEC = 6 or 4, and a regular ring for FEC = 8. These rules agree well with the experimental geometries found for a variety of $[M_2(\mu\text{-}XR_2)_2L_8]$ complexes with different metal atoms. Our calculations with terminal chloride ligands, however, suggest that steric factors may in some cases destabilize the electronically preferred structure with short metal−metal distance.

For NRE ≤ 18, a second structure is predicted with a short through-ring X−X distance. Although such structures are expected to be higher in energy, in agreement with the nonexistence of structurally characterized compounds, they appear to be an interesting possibility and a search for ways to stabilize them should be worth of future theoretical and experimental work. In particular, our qualitative analysis predicts that for NRE = 6 the structure with short X−X distance is slightly more stable than that with a short M−M distance. A few structurally characterized complexes with short X−X distances have been reported, although they have a different number of terminal ligands than those considered in the present study.

For complexes with methyl and isolobal bridges, only two framework bonding orbitals can be formed and a net M−M bonding interaction is predicted for any number of ring electrons between 4 and 16. These correspond to occupation of the two framework bonding and the six t_{2g}-block orbitals, hence to FEC = 4 in all cases. Two remarkable differences with XR_2-bridged analogues appear: (i) in the present case, even for formally d^6 metal ions, the most stable structure is that with a short metal−metal distance; (ii) in XR_3-bridged compounds, the alternative structure with short X−X distance is unstable. For such complexes, a population analysis indicates that most of the metal−metal bonding interaction should be attributed to a delocalized interaction involving the four atoms of the M_2X_2 ring, with a small contribution of the direct σ-type interaction between the t_{2g} orbitals of the two metal atoms. It must be stressed that for compounds such as $[Re_2(\mu\text{-}H)_2(CO)_8]$ or $[Os_2(\mu\text{-}H)_2(PR_3)_6(H)_2]$, formally d^6 complexes, no metal−metal bonding should be expected based on the t_{2g}^6 configuration of the metal atoms, yet the framework electron counting rules correctly predict short metal−metal distances as experimentally found (2.876 and 2.818 Å, respectively).

Let us now try to extend our conclusions to the analysis of bonding in the mixed binuclear complexes of the type $[L_4M(\mu\text{-}XR_n)_2M'L_2]$ (**7**),

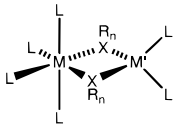

7

where M′ may appear in either a tetrahedral or square planar $M'X_2L_2$ geometry. We recall here that in our previous studies of through-ring bonding in M_2X_2 cores of square planar[3] (or tetrahedrally[2]) coordinated metal ions we showed that eight (or ten) d-electrons per metal atom do not participate in the framework bonding, and thus only the electrons provided by the bridging ligands, together with any additional metal electrons, must be included in the framework electron count (FEC). In the present work we have devised a simplified electron counting scheme for octahedrally coordinated metal atoms. According to such a scheme, the lowest six ring electrons have framework bonding (φ) character and only when the t_{2g} orbitals are occupied is the fourth φ orbital occupied. We can now deduce which electron counts in mixed edge-sharing binuclear complexes with two different ML_n fragments will give rise to FEC = 6 or less and therefore to short through-ring metal−metal distance (Table 5).

A structural database search indicates that all such complexes with NRE of 20 or less (10 structures retrieved from the Cambridge Structural Database) have short metal−metal distances, as revealed by Δ_{MM} values of less than 0.2 Å. The only

Table 5. Number of Ring Electrons (Metal d and Bridging Ligand Lone Pairs, NRE) Corresponding to Six Framework Electrons (FEC = 6) for Different Combinations of ML_n Fragments in Edge-Sharing Binuclear Compounds with M_2X_2 Cores

	ML_4 (octahedral)	ML_2 (square planar)	ML_2 (tetrahedral)
ML_4 (octahedral)	18	20	22
ML_2 (square planar)		22	24
ML_2 (tetrahedral)			26

[a] For these electron counts, a short through-ring M−M distance should be expected.

apparent exception[43] corresponds to a complex with one tetrahedrally coordinated Fe(II) ion for which one cannot assume the closed shell d^{10} configuration. Those compounds with 24 ring electrons, for which a FEC of 8 is expected (i.e., two more electrons than shown in Table 5), have Δ_{MM} larger than 0.3 or 0.2 Å when the bridging atoms are sulfur[44−47] or oxygen,[48−51] respectively. These data, together with the acute X−M−X angles (the average for the two metal atoms in the M_2X_2 ring is smaller than 80°), indicate that such through-ring distances must be considered as nonbonding.

For those compounds with NRE = 22, two alternative structures exist. The tetracoordinate metal may be in a square planar environment, for which the number of framework electrons is eight, and no short through-ring distance is to be expected. However, if the tetracoordinate metal has a tetrahedral coordination sphere, only six out of the 22 ring electrons occupy framework bonding orbitals (FEC = 6) and a short metal−metal distance is predicted. The experimental structural data nicely confirm these simple rules, with the compounds **7** having $\Delta_{MM'}$ larger than 0.2 Å when M′ is close to square planar[52−55] but negative when M′ is nearly tetrahedral.[56−58]

The structure of type **2c** with a short X−X distance seems to be possible for compounds with NRE = 18 or less, although the present calculations indicate it to be higher in energy than that with a short M−M distance (**2a**). A variety of such complexes exist with N−N, O−O, C−C or Si−Si short through-ring distances, but none of them with ML_4 groups. Theoretical and experimental search for the factors that may stabilize such a structure seems therefore highly desirable.

An interesting extension of the present ideas is suggested by recent theoretical work of Bénard and co-workers[14] on the M_2X_2 ring in an edge-sharing square pyramid of the reduced Keggin heteropolyanions γ-$[SiW_{10}M_2X_2O_{38}]^{6-}$ (M = Mo, W; X = O, S). Both DFT calculations and experiment show a short M−M distance, consistent with the bonding scheme **2a** in that ring, as would be expected for NRE = 10. In addition, the DFT calculations detect the existence of energy minima in which two electrons are transferred from the M_2X_2 core to the decanuclear skeleton $SiW_{10}O_{36}$, with the subsequent change in NRE and an increased M−M distance corresponding to structure **2b**.

Acknowledgment. Financial support to this work was provided by Dirección General de Enseñanza Superior (DGES) through Grant PB98-1166-C02-01. The authors thank E. Ruiz for many helpful discussions and M. Bénard for providing them with a preprint of unpublished work.

Appendix

Molecular orbital calculations of the extended Hückel type[59−61] were carried out using the modified Wolfsberg−Helmholz formula[62] on model compounds with different NREs. Standard atomic parameters[61,63] were used for the extended Hückel calculations. The following bond distances and angles were used for the bridging ligands: Cr−N = 2.030, Cr−P = 2.318, Cr−C = 2.188, N−H = 1.010, P−H = 1.415, C−H = 1.050 Å; H−N−H = H−P−H = H−C−H = tetrahedral angles. For the terminal ligands, the following bonding parameters were used: Cr−C = 1.870, Cr−H = 1.600, Cr−Cl = 2.290, C−O = 1.145, Cr−Cp centroid = 1.876, C−C = 1.399, C−H = 1.050 Å; Cr−C−O = 180.0, and L−Cr−L = 90°. The search for experimental structural data was carried out with the help of the Cambridge Structural Database.[64] Searches were performed for any transition metal with XR_2 bridges, being X any group 14, 15, or 16 element. The terminal ligands were allowed to be an η^5-cyclopentadienide ring or any group linked to the transition metal through a donor atom of groups 14−17.

The atomic radii for transition metal atoms were obtained by subtracting the atomic radii of N (0.68 Å) from the average of the M−N(sp^3) bond distances in the Cambridge Structural Database. To avoid the long distances associated with the Jahn−Teller effect in Cu(II), only M−N distances corresponding to tetracoordinate Cu atoms were considered. Similarly, to rule out long distances associated with compounds with more than 20 valence electrons, the search for Zn, Ag and Au was restricted to coordination numbers 2 or 4. The resulting atomic radii are included as Supporting Information, together with the number of experimental data and the standard deviation of the sample.

Density functional calculations were carried out using the GAUSSIAN94 package.[65] The hybrid B3LYP-DFT method was

(43) Queisser, J.; Oesen, H.; Fenske, D.; Lehari, B. *Z. Anorg. Allg. Chem.* **1994**, *620*, 1821.
(44) McCleverty, J. A.; McLuckie, S.; Morrison, N. J.; Bailey, N. A.; Walker, N. W. *J. Chem. Soc., Dalton Trans.* **1977**, 359.
(45) Healy, P. C.; Skelton, V. W.; White, A. H. *J. Chem. Soc., Dalton Trans.* **1989**, 971.
(46) Konno, T.; Yoshinari, Y.; Okamoto, K. *Chem. Lett.* **1995**, 989.
(47) Brooker, S.; Croucher, P. D. *J. Chem. Soc., Chem. Commun.* **1995**, 2075.
(48) Glick, M. D.; Lintvedt, R. L.; Anderson, T. J.; Mack, J. L. *Inorg. Chem.* **1976**, *15*, 2258.
(49) Brewer, G. A.; Sinn, E. *Inorg. Chem.* **1987**, *26*, 1529.
(50) Nanda, K. K.; Das, R.; Venkatsubramanian, K.; Paul, P.; Nag, K. *J. Chem. Soc., Dalton Trans.* **1993**, 2515.
(51) O'Bryan, N. B.; Maier, T. O.; Drago, R. S. *J. Am. Chem. Soc.* **1973**, *95*, 6640.
(52) Thewalt, U.; Muller, S. *Z. Naturforsch.* **1989**, *44b*, 1206.
(53) Konno, T.; Machida, T.; Okamoto, K. *Bull. Chem. Soc. Jpn.* **1998**, *71*, 175.
(54) Durán, N.; González-Duarte, P.; Lledós, A.; Parella, T.; Sola, J.; Ujaque, G.; Clegg, W.; Frasser, K. A. *Inorg. Chim. Acta* **1997**, *265*, 89.
(55) Shimada, S.; Tanaka, M.; Honda, K. *J. Am. Chem. Soc.* **1995**, *117*, 8289.
(56) Flörke, U.; Haupt, H.-J. *Acta Crystallogr., Sect. C: Cryst. Struct. Commun.* **1993**, *49*, 1906.
(57) Coutinho, K. J.; Dickson, R. S.; Fallon, G. D.; Jackson, W. R.; de Simone, T.; Skelton, B. W.; White, A. H. *J. Chem. Soc., Dalton Trans.* **1997**, 3193.
(58) Fischer, K.; Vahrenkamp, H. *Z. Anorg. Allg. Chem.* **1981**, *475*, 109.
(59) Hoffmann, R.; Lipscomb, W. N. *J. Chem. Phys.* **1962**, *36*, 2179.
(60) Hoffmann, R. *J. Chem. Phys.* **1962**, *37*, 2872.
(61) Hoffmann, R. *J. Chem. Phys.* **1963**, *39*, 1397.
(62) Ammeter, J. H.; Bürgi, H.-B.; Thibeault, J. C.; Hoffmann, R. *J. Am. Chem. Soc.* **1978**, *100*, 3686.
(63) Summerville, R. H.; Hoffmann, R. *J. Am. Chem. Soc.* **1976**, *98*, 7240.
(64) Allen, F. H.; Kennard, O. *Chem. Des. Autom. News* **1993**, *8*, 31.
(65) Frisch, M. J.; Trucks, G. W.; Schlegel, H. B.; Gill, P. M. W.; Johnson, B. G.; Robb, M. A.; Cheeseman, J. R.; Keith, T. A.; Petersson, G. A.; Montgomery, J. A.; Raghavachari, K.; Al-Laham, M. A.; Zakrzewski, V. G.; Ortiz, J. V.; Foresman, J. B.; Cioslowski, J.; Stefanov, B. B.; Nanayakkara, A.; Challacombe, M.; Peng, C. Y.; Ayala, P. Y.; Chen, W.; Wong, M. W.; Andrés, J. L.; Replogle, E. S.; Gomperts, R.; Martin, R. L.; Fox, D. J.; Binkley, J. S.; Defrees, D. J.; Baker, J. P.; Stewart, J. P.; Head-Gordon, M.; Gonzalez, C.; Pople, J. A., *Gaussian 94*, Revision E.1; Gaussian, Inc.: Pittsburgh, PA, 1995.

applied, in which the Becke three parameters exchange functional[66] and the Lee−Yang−Parr correlation functional[67] were used. The double-ζ basis set for the valence and outermost core orbitals combined with pseudopotentials known as LANL2DZ were used for all the atoms.[68,69] The geometries were fully optimized using gradient techniques and symmetry restrictions were introduced in the optimizations when possible. Attempts to obtain broken-symmetry solutions of the low spin states were unsuccessful and converged to the singlet state for the structures **2a** and **2c** of $[Cr_2(\mu\text{-}PH_2)_2(CO)_8]$.

(66) Becke, A. D. *J. Chem. Phys.* **1993**, *98*, 5648.
(67) Lee, C.; Yang, W.; Parr, R. G. *Phys. Rev., B* **1988**, *37*, 785.
(68) Dunning, T. H., Jr.; Hay, P. J. *Modern Theoretical Chemistry*; Plenum: New York, 1976; p 1.
(69) Hay, P. J.; Wadt, W. R. *J. Chem. Phys.* **1985**, *82*, 299.

Supporting Information Available: Tables listing refcodes, NREs, M−M distances, and Δ_{MM} values for all structures represented in Figure 6, and table of atomic radii for transition metal atoms adopted in the calculation of Δ_{MM}, together with pertinent statistical data. This material is available free of charge via the Internet at http://pubs.acs.org.

IC000017I